Technical Note BN-407 October 1965

ATOMIC PROCESSES IN PLASMAS*

by

T. D. Wilkerson

University of Maryland
College Park, Maryland

*Research initially supported by U.S. Air Force Office of Scientific Research; now supported by the Office of Space Science and Applications, NASA, through grants NsG-283 and NsG-359.

ABSTRACT 26698

Experimental plasma physics deals both with atomic and collective processes, i.e., with two- and three-body interactions of particles and photons vs. many-body interactions over distances of order a Debye length or cyclotron radius. Two of the Institute's laboratories are engaged in measuring atomic radiation and collision coefficients which are important in stellar atmospheres, dilute plasmas in space, and high temperature plasmas on earth.

Radiative transition probabilities will be measured for spectral lines of several light elements; e.g., CI, CII, SI, SII, NeI, AI, AII, between 2000 and 12000 Å. Other elements and shorter wavelengths will follow this initial program. The spectroscopic source is a gas-driven shock tube which operates up to 15000°K with at least 100 microseconds of steady conditions behind the reflected shock. Particular attention has been paid to direct measurement of the gas properties, rather than relying on shock wave theory alone. Data are presented on excitation temperature, measured by the line-reversal technique. The flash lamp and fibre-optics employed for this and other purposes are also described.

ATOMIC PROCESSES IN PLASMAS*

T. D. Wilkerson

Institute for Fluid Dynamics and Applied Mathematics

University of Maryland
College Park, Maryland

I. Introduction

Events taking place at the atomic level of matter are not only of great interest in themselves, but also important on a larger scale where they can both influence the behavior of many-particle systems and often tell us what is going on in these systems. This is particularly true in plasmas, where the light emitted by constituent atoms, ions and electrons contains a great deal of information about the plasma state, and this state is governed by collision interactions of particles which may have been accelerated by plasma waves or other large scale events. This interplay between few-particle and many-particle phenomena is important in space plasmas, such as the earth's ionosphere, comet tails, and as far as we know all zones of the atmospheres of the sun and other stars. In earth bound plasmas, and high temperature gases generally, we can find examples in controlled or uncontrolled fusion devices, rocket exhausts, MHD power generators, and the plasmas used for basic research such as those described in this session by Dr. Lashinsky and by Dr. Kolb.

---

*Research initially supported by U.S. Air Force Office of Scientific Research; now supported by the Office of Space Science and Applications, NASA, through grants NsG-283 and NsG-359.

A specific case of great interest is the stellar plasma, which sends its light to us over great distances -- an elaborate code describing what elements are present and how much of each, the density of electrons, the temperature (if it can be defined) and variations of all these quantities in space and time. Reading this code requires that we know the atomic constants governing both radiation and collision; the better one can read it, the more can be said about the abundances of the elements on a universal scale and the probable evolution of the universe.

Two of the Institute's laboratories are studying atomic processes of interest in plasma physics. The first category I will discuss in Section 2 is heavy particle collisions, currently between 100 and 1000 electron volts and later on as low as we can achieve, hopefully in the 1 to 10 eV range. Several topics are currently under study but the furthest advanced is the measurement of electron capture by hydrogen ions in various gases. The bulk of this work has been done by Dr. D. W. Koopman, Mr. P. G. Cable, and Mr. M. Kato -- with the assistance of Dr. K. W. Ogilvie (Goddard Space Flight Center), Mr. H. J. Zwally, Mr. J. Brecht and myself.

Section 3 will treat the current state of research on transition probabilities for atomic line radiation, or more precisely the first results of the plasma-diagnostic procedures being applied to the shock tube which is our spectroscopic source. This gas-driven shock tube easily achieves temperatures up to $15000^{o}K$ and electron densities up to 10^{17} cm^{-3}, so that many lines of light elements can be observed both in emission and

absorption, under known conditions. The principal researchers have been Dr. G. Charatis, Mr. M. H. Miller and Mr. G. Mabry, and assistance has come from Dr. D. W. Koopman and myself, Mr. P. W. Murphy, Mr. J. R. W. Hunter and Mr. S. McPhillips.

II. Collision Cross Sections

Heavy particle interactions form an important, and sometimes dominant, class of events in plasmas, and are very hard to treat theoretically. One realizes at the outset that a complete description of two atomic systems in collision must, at least in some ranges of energy, reckon with molecular properties, namely the properties of the molecule capable of even a transient existence in the collision. Moreover, the generally high rate of approach of the collision partners makes it unclear what molecular problem to solve. Since the customary hierarchy of energy level types (Born-Oppenheimer approximation) is turned over, one is left with only rough ideas as to what to expect [1,2,3]. An early attempt at an overall view was Massey's "adiabatic criterion"[4] which predicts maximum charge-exchange cross sections for that energy which makes the collision duration comparable to a quantum mechanical transition time, $h/\Delta E$, where h is Planck's constant and ΔE is the energy change or extent of inelasticity in the collision process. This idea is borne out by a striking number of cases of charge-exchange[4].

The experiments reported below are in the transition region between non-adiabatic and adiabatic (sufficiently slow collisions that

atoms smoothly adjust to each other's presence). This energy range is most important to understand well, though it falls below many cross-section maxima, because (i) reaction rates between species in a plasma are integrals of cross-sections weighted by particle distribution functions, and (ii) most plasmas have distribution functions which peak in or below this energy range.

We have begun to study several types of heavy particle collisions (single ion - atom, single ion - molecule, multiple ion - atom) while pursuing one type to the place where the results can be compared with previous work. We report here the latter results on electron capture by H^+ and H_2^+ in argon in the energy range 100 - 1000 eV, while indicating some of the developmental work that has gone before[5].

Figure 1 shows a typical system in which an ion beam can be generated, analyzed, controlled and detected. This top view shows two diffusion pumps and a bell-jar as the main vacuum components. From left to right we have an electron-bombardment ion source[6,7], a "Wien filter" or $\vec{E}x\vec{B}$ velocity selector, an electrostatic energy analyzer[8] and a detector[9] capable of recording single ions even at energies of leV.

This system has proved very useful for learning how to carry out beam operations properly and for testing various components. Several modifications stand between it and the hydrogen-argon measurements, but not such drastic ones as to vitiate the experience gained here.

Figure 2 shows the combined energy -- velocity analysis of the ion beam in the prototype system, where the data points correspond to

simultaneous settings of the energy analyzer and velocity selector. The three mass groups evident here are H^+, H_2^+ and heavy particles such as N_2^+; each follows the expected relation between particle energy and velocity-squared. This graph shows that we could in principle use either the proton or H_2^+ beams for meaningful collision experiments over the indicated energy range.

As a practical matter, however, the ion currents here were too low for the type of scattering geometry to be used first, so that a higher current, RF ion source (ORTEC) was used. Radio frequency ion sources are commonly employed in van de Graaf accelerators and typically consume tens of watts of RF power in the frequency range of tens of megacycles. In the energy range of interest to us, typical total ion-output currents were in the range 1 - 10 microamperes; the source has magnetic focussing and is electrically isolated for greater control over the mean particle energy. Careful shielding is required to keep rectified RF out of oscilloscopes and sensitive electrometer circuits.

Electrometers are used for measuring currents in the scattering chamber shown in Figure 3. This chamber[10,11] takes the place of the single-ion detector on the right of the bell-jar in Figure 1. Its purpose is to provide a low pressure gas target for the main beam in such a way that cross-currents due to scattering can be collected while the rest of the vacuum system is at a sufficiently low pressure as not to perturb the ion beam. Typically we would have a 500-eV proton beam entering this chamber through

the slit below, and the internal chamber pressure would be about one micron (10^{-3} Torr) of argon. Two principal reactions ensue: the one of interest here is electron capture by the proton, yielding a fast neutral hydrogen atom, plus a slow argon ion which is easily swept up by the weak electric field put across the chamber. The electron capture cross section is given by the ratio of scattered-to-incident currents, divided by the number of argon scattering centers per cm^2 in the "line of sight" of a typical proton. The other important reaction to consider is ionization, which could contribute spurious effects to electron capture measurements; however, an ionizing proton will simply create an electron-argon ion pair and continue on through the chamber with slightly reduced energy. Both the electron and ion will be collected, so that neither will contribute to the net positive current observed flowing to the collection plates. In other words, we are using the chamber in a mode which balances out ionization currents, leaving only the electron-capture contribution. Almost needless to say, this mode of operation requires great caution about collection of charged particles, production of secondary electrons, etc. The scatter in our results probably reflects our degree of control over these effects at the time the data were collected.

At a given proton or H_2^+ energy, the electron-capture current I_c and the main beam current I_o are measured as functions of chamber pressure, so that zero-levels can be subtracted away (due to leakage current in the scattering chamber) and that the thinness of the gas target can be verified. Figure 4 shows data for H^+ and H_2^+ over a range of incident

ion energies, and illustrates the method of data reduction already alluded to. Each of our data boxes contains 4 to 8 different pressure runs by various operators. The widths of the boxes are not due to uncertainities in energy, but indicate rather the energy spread in groups of results chosen for averaging together; the scatter of results even at one energy was comparable to what is shown here (20-25%).

The proton data are similar to earlier results,[11,12,13] but suggest a stronger dependence of the cross section on energy than has been seen before. The matter is clouded by a degree of scatter which is quite common in cross section experiments. Probable error is often not clearly specified in the literature, but the scatter of all these measurements seems to be comparable to ours. Our immediate plans are to reduce the random errors due to background gas and leakage currents, and to examine several rare gases for significantly steeper cross section curves than have been measured before. As implied early in this section, such results would seriously affect calculated reaction rates for charge exchange in plasmas having most of their particles in the lower energy range under discussion.

As for the H_2^+ results, we cannot yet make a clear comparison because of the possibilities of beam contamination due to H_3^+ or excited states of H_2^+; the latter feature may also affect the earlier work. It is now fairly widely realized that many absolute cross section measurements have been influenced to an uncertain degree by atomic excitation, so that redeterminations by factors of 2 and 3 would not be surprising. We expect to return to the study of molecular hydrogen ions after completing beam-manipulation sections for higher H_2^+ purity and longer times of flight.

Our present data on H_2^+ may be affected by the production of secondary electrons[14] to a degree which may require more elaborate precautions.

In this section we have seen that there is a great practical need for good cross section data, particularly at low energy, and that there is an intrinsic physical interest particularly for heavy particle interactions. That charge-exchange cross sections rise rapidly to maxima in the kilovolt range seems to be due to the mutual interaction of many particles which, so to speak, do not have time to adjust to the rapid onset of perturbation. To pass beyond a picturesque description to a grasp of the simultaneous quantum processes involved has proved to be very difficult. Further experimental work - particularly at low energy - seems mandatory in view of the theoretical difficulties and experimental disagreements.

III. Atomic Transition Probabilities

We are measuring atomic transition probabilities, using a gas-driven shock tube as a spectroscopic source. Since such instruments can generate a plasma of known conditions and composition, and our observing instruments record atomic line intensities, one has only to divide, as it were, the line intensity by the number of atoms in the upper energy level in order to find the inherent probability (per atom in the excited state) for the line to be emitted. Once in possession of such atomic constants for a given element, an astrophysicist can use the line intensity seen in a distant source as a measure of the elemental abundance in that source. Reliable calculation of line strengths is still difficult in general, so empirical determination of them is desirable, at the very least, and

mandatory in many cases.

General accounts of this type of experimental astrophysics have appeared in recent years[15-19], and the shock tube has played a prominent role in this field[20-24]. Our present emphasis is on the spectra of the light elements (e.g., neutral and singly-ionized carbon and sulphur), between 2500 and 10,000 Å, on new diagnostic techniques and instrumentation, and on preparations for future work in the vacuum ultraviolet. We report here the first results of experiments to check on plasma conditions in the shock tube. In refined form, these will be coupled with line-intensity measurements to give the final data on atomic transition probabilities. For this purpose, the shock tube has two great advantages over many other light sources: the plasma possesses a high degree of uniformity along a line of sight perpendicular to the tube axis, and there exists a well defined and extensive theory for the plasma state to be achieved as a function of shock velocity.

Figure 5 shows the shock-reflection end, or "test-section", of our shock tube. When the tube is fired by release of the high pressure "driver gas" several meters upstream, a shockwave runs through the test gas into this chamber and reflects from the end wall. Having thus been twice compressed by strong shock waves, the test gas is elevated in temperature to 10,000-15,000°K and rendered highly luminous. It is stationary at these conditions for about 100 microseconds. Subsequent wave interactions further increase the gas temperature, so that one would see here a succession of thermodynamic states which must be time resolved in order that we have a well defined state for spectroscopic analysis.

Typical time-resolved emission spectra are shown in Figure 6, with time increasing downward and wavelength increasing from the blue (left) to the red (right). The bulk of the test gas is neon in both cases, while we have added of order 1% H_2S and CH_4 in the upper and lower experiments, respectively. In both, then, we naturally see the blue-green Balmer line H_β (4861 Å) and the familiar red lines of neon. There is an evident time-development toward brighter spectra and hotter states, as multiply-reflected shocks compress the gas behind the first reflected shock wave. The quenching of luminosity is due to mixing with the cold driver gas which finally expands down the entire length of the shock tube. Prior to any atomic emission, one sees the Swan bands of C_2 at the primary and reflected shock waves[25] when methane is used as the spectroscopic additive.

Behind the first reflected shock in the methane case, we see characteristic lines of atomic carbon at 5380 Å, 5052 Å, etc. They are absent when hydrogen sulphide is used; instead we then see strong lines of neutral sulphur, such as 4695 Å and more diffuse members of the same multiplet.

We have made a great number of hydrodynamic measurements which verify that the gas behind the first reflected shock is close to the thermal state predicted by shock wave theory. These include reflected shock velocity and absolute pressure, and extend the range of previous checks of this type[16]. The absolute pressure in question is usually about 10 atmospheres, and the temperature above 10,000°K - conditions which, together with the amount of spectroscopic additive, usually guarantee a steady state in local thermodynamic equilibrium, even though the available times are in the 100 microsecond range.

Passing to spectroscopic measurements of the plasma state, already one such is implicit in the diffuse character of the H_β lines which is evident in Figure 6. The hydrogen atom, being a one-electron system, is particularly susceptible to the Stark effect - which manifests itself here as a broadening related directly to the density of charged particles in the gas[19]. Toward the end of this section, I will discuss the methods we are using to measure electron density from the H_β profile. For now it should suffice to point out that such measurements do indeed provide a check on the ionization temperature of the shock tube plasma.

A direct measurement of excitation temperature is provided by the method of spectral line-reversal[26]. Imagine that a very bright (and variable) source of continuous radiation be placed behind the shock tube test section in Figure 5. Given the appropriate windows, a spectroscopically equipped observer on the near side of the tube would see emission spectra of the type shown in Figure 6 only if the background radiation were held down to a low level. If the background continuum were then turned up, so to speak, so that its brightness exceeded the Planck (black body) function appropriate to the shock tube temperature, our observer would then see the shock tube spectra in absorption against the intense background. By so adjusting the external source that one finds the reversal point from bright-line to dark-line spectra, one puts in evidence the shock tube's Planck function - which is to say its temperature - without recourse to any atomic constants save the velocity of light and Planck's constant.

This is accomplished with our shock tube by means of a very bright, pulsed flash lamp[27,28], whose continuum intensity varies in times suitably

short that reversal can be clearly observed once or several times during the 100 microsecond interval of interest. Essentially what one measures is the population ratio of the two atomic energy levels associated with the given spectral line. A good test of the customary equilibrium assumptions is that all lines of all elements shall demonstrate reversal at the same temperature and that this temperature shall correspond to the ionization and gas-kinetic temperatures found by other means.

The first line-reversal results in the present program are shown in Figure 7. In the lower graph, reversal temperatures for neon lines behind the first reflected shock are compared to the temperatures predicted from shock tube theory and the primary shock Mach number. Though the method is not precise, owing to low optical depth in the lines studied, the results are definitely in the range hoped for. Much more precise measurements are now underway, in conjunction with definitive hydrodynamic calculations of real gas effects. As far as we are aware, these reversal measurements in the range 10,000-15,000^{o}K are pioneering ones; we expect them to yield much valuable data in this and other laboratories. Given sufficient precision, they may offer the possibility of cross checking the radiative and thermal temperature scales in this range.

Furthermore, the upper graph of Figure 7 suggests that useful gaseous states well above 15,000^{o}K may be attained, in the same experiments, behind multiply-reflected shock waves. Of course it remains to be shown that this region is so free of inhomogeneities as the well-formed plasma behind the reflected shock. This too will be looked into further.

The present data on line-reversal also exemplify a trend in our work, namely to augment photographic procedures with multi-channel photoelectric recording. With conventional shock tubes, which cannot profitably be fired at one-minute intervals, photographic spectroscopy is practically essential for recording wide spectral ranges; its main drawback is the requirement of absolute, heterochromatic photodensitometry of films, which is tedious and gives intensity precisions of 5% at best. With several photoelectric channels, one can easily record a chosen subset of the data under higher precision without, however, depending solely on wavelength scans over a long series of experiments. The reversal measurements were made by means of slitted "light pipes" in the spectrographic image plane, each feeding its own photomultiplier. Some of the fiber bundles were located on spectral lines and others in the line-free continuum between.

Spectral line profiles are also recorded with a multi-channel photoelectric device shown in Figure 8 (this is called a SQUID, for sequential image dissector). The essential feature of this device is that the clean geometry of a microscope cover-glass is combined with light pipe flexibility, so that many narrowly-spaced wavelength bands can be observed by a set of photomultipliers. Figure 8 shows the squid model now in use; the data given here were taken with a prototype that required considerable compensation for differing angular properties of the channels.

To check the operating principle of the squid, one channel was studied with the usual laboratory light sources and then tuned over the H_β profile during the course of several similar shock tube runs. The results

are shown in Figure 9. Then the first multichannel squid was assembled and used in many experiments; two typical runs are given in Figure 10. In all cases one can fit the data to expected profiles and thereby estimate the electron densities from the halfwidths[19]. These estimates are indeed comparable to calculated electron densities for shock tube runs of this type, so we have confirmed the expected range of conditions from yet another point of view. Further observations and developments with squid devices will soon be reported[30].

In this section, we have seen that the conventional shock tube gives high temperature results for electron density and temperature that are within 20% of expectations. Thus an important step is made towards the study of light elements and their ions under those conditions. The necessary improvements of instruments are clear and are underway, so that new line-strength data will soon be available on such elements as sulphur, carbon and the halogens. We expect that these data will be useful for checking approximate methods of calculating line strengths and for measuring plasma conditions and elemental abundances in a variety of light sources.

IV. Conclusion

The Institute's experimental studies of collisional and radiative processes at the atomic level will continue along those lines of importance in understanding laboratory and astrophysical plasmas. Ample evidence exists for the dual character of plasma physics as a scientific discipline. It is generally true that both two-body and collective particle interactions must be understood in order to have a complete picture, while one type of

process or the other may dominate in any particular case. Together with the Institute's theoretical and experimental studies of collective processes, we expect the atomic experiments introduced here to contribute valuable data for future developments in plasma physics.

REFERENCES

1. E. W. McDaniel, Collision Phenomena in Ionized Gases, John Wiley (1964) particularly Chapter 6.

2. J. B. Hasted, Physics of Atomic Collisions, Butterworths (1964) particularly Chapter 12.

3. J. W. Bond, K. M. Watson, and J. A. Welch, Atomic Theory of Gas Dynamics Addison-Wesley (1965) particularly Chapter 4.

4. H. S. W. Massey, Rep. Prog. Phys. 12, 248 (1949); J. B. Hasted, Advanc. in Electronics and Electron Phys. 13, 1 (1960).

5. P. G. Cable for the Atomic Collision Group, "Atomic Collision Research", University of Maryland Technical Note BN-404 (June, 1965).

6. N. D. Coggeshall and E. B. Jordan, Rev. Sci. Instr. 14, 125 (1943).

7. H. D. Hagstrum, Rev. Sci. Instr. 24, 1122 (1953).

8. A. L. Hughes and V. Rojansky, Phys. Rev. 34, 284 (1929).

9. W. Schütze and F. Bernhard, Zeit. für Phys. 145, 44 (1956).
   N. R. Daly, Rev. Sci. Inst. 31, 264, 720 (1960).
   V. V. Afrosimov, I. P. Gladkovskii, Yu S. Gordeev.
   I. F. Kalinkevich and N. V. Fedorenko, Soviet Phys.-Tech. Phys. 5, 1378, 1389 (1961).
   H. P. Eubank and T. D. Wilkerson, Rev. Sci. Instr. 34, 12 (1963).
   K. W. Ogilvie, N. McIlwraith, H. J. Zwally and T. D. Wilkerson, NASA Technical Note, NASA TN D-2111 (1964).

10. J. B. Hasted, Proc. Roy. Soc. A205, 421 (1951).

11. J. B. Hasted, Proc. Roy. Soc. A212, 235 (1952).

12. F. Wolf, Ann. Phys. Lpz. 23, 185, 627 (1936); 25, 527, 737 (1936).

13. J. B. Hasted and J. B. H. Steddeford, Proc. Roy. Soc. A277, 466 (1955).

14. S. N. Ghosh and W. F. Sheridan, J. Chem. Phys. 26, 480 (1957).

15. H. E. Petschek, P. H. Rose, H. S. Glick, A. Kane and A. Kantrowitz, J. Appl. Phys. 26, 83 (1955).

16. O. Laporte and T. D. Wilkerson, Journ. Opt. Soc. Am. 50, 1293 (1960).

17. A. C. Kolb and H. R. Griem, "High Temperature Shock Waves", Chapter 12 in Atomic and Molecular Processes (D. R. Bates, Ed.) Academic Press (1961).

18. W. L Wiese, Proceedings of the Tenth Colloquium Spectroscopicum Internationale (E. R. Lippincott and M. Margoshes, Ed.) p. 37, Spartan Books, Washington, D. C. (1963).

19. H. R. Griem, Plasma Spectroscopy, McGraw-Hill (1964).

20. G. Charatis and T. D. Wilkerson, Phys. Fluids 5,1661 (1962); Proceedings of the Sixth International Conference on Ionization in Gases, Vol. III, p. 401, SERMA, Paris (1963).

21. S. H. Bauer, J. H. Kiefer and B. E. Loader, Can. J. Chem. 39, 1113 (1961).

22. D. W. Koopman, Phys. Fluids 7, 1951 (1964); Journ. Opt. Soc. Am. 54, 1354 (1964).

23. R. C. Elton and H. R. Griem, Phys. Rev. 135, A1550 (1964); R. A. Day and H. R. Griem, Phys. Rev. 140, A1129 (1965).

24. W. R. S. Garton, W. H. Parkinson and E. M. Reeves, Ap. J. 140, 1269 (1964). L. Goldberg, W. H. Parkinson and E. M. Reeves, Ap. J. 141, 1293 (1965).

25. G. Charatis, L. R. Doherty and T. D. Wilkerson, J. Chem. Phys. 27, 1415 (1957).

26. F. Kurlbaum, Phys. Z. 3, 189 (1902); Fery, Compt. Rend. 13, 909 (1903); H. Kohn, Phys. Z. 33, 957 (1932).

27. W. R. S. Garton, J. Sci. Instr. 30, 119 (1953).
W. R. S. Garton and A. Rajaratnam, Proc. Roy. Soc. (London) A70, 815 (1957); W. R. S. Garton, J. Sci. Instr. 36, 1 (1959).

28. G. Charatis and T. L. Hershey, "A Flash-Lamp Source of High Intensity Continuous Spectra", Univ. of Md. Technical Note BN-361 (July 1964).

29. G. Mabry and G. Charatis, to be published.

30. M. H. Miller, T. D. Wilkerson and J. R. W. Hunter, Proceedings of the Culham Conference on UV and X-Ray Spectroscopy of Plasmas, Institute of Physics, London (1965).

FIGURE CAPTIONS

Figure 1 Apparatus for producing and analyzing ion beams. From left to right, A and B show the electron-bombardment ion source, C a compound lens. P_1 a pump-port, V a crossed-field velocity selector ($\vec{E} \times \vec{B}$), D two pairs of deflection plates, C another lens, P_2 the main pumping port, E a cylindrical electrostatic energy analyzer, and K, F, S components of a single-ion detector. This apparatus was very useful for energy and mass analysis of beams and for systematic studies of beam current and geometry.

Figure 2 Simultaneous energy-velocity analysis of ions emitted by electron-bombardment source running on hydrogen gas. Data collected by setting repeller voltage in ion source, finding the roughly equivalent energy analyzer voltage, then tuning the potential drop in the velocity selector (left-hand ordinate) to the peaks in observed ion current. The ion groups shown here are, in ascending order, H^+, H_2^+ and $O_2^+ - N_2^+$. The minimum observable ion energies were about 40 eV for H_2^+ and 140 eV for H^+. Ion beam width at entrance to energy analyzer roughly 1 cm.

Figure 3 Gas cell for observing ionization and electron-capture currents due to primary ion beam passing through the gas. Cross-currents are measured as functions of primary beam type, current and energy and of gas pressure.

Figure 4 Absolute electron-capture cross sections for H^+ and H_2^+ in argon, measured as indicated in text and in figure on right. Proton results suggest steeper energy dependence than observed in earlier work. Reliability of H_2^+ results in doubt, due to possibilities of beam contamination and unaccounted-for secondary electron emission.

Figure 5 Test section of spectroscopic shock tube with 1-ft. scale. Tube is 3" x 4" welded tube with inside seam removed; wall thickness 3/16". Reinforcement with bars and jigs prevents elastic deformations due both to shock pressures and to the static pressures (500 - 1000 psi) following each experiment. Mountings for side windows and transducers are shown. "Driver gas" chamber (4 meters upstream) not shown.

Figure 6 Time-resolved emission spectra recorded near end of shock tube, using f/6.3 spectrograph and rotating-drum camera. Shock tube test gas is neon plus "spectroscopic additive"; additive was H_2S in upper picture and CH_4 in the lower. Direction and extent of arrows show the time direction and duration of the state behind the first reflected shock. Hydrogen and red neon lines appear in both films, while the upper shows one of the strong lines of neutral sulphur (4695 Å), the lower several lines of neutral carbon and molecular bands of C_2. Hotter gases at later times yield brighter and wider lines and an enhanced recombination continuum.

Figure 7 Comparison of predicted and observed line-reversal temperatures, demonstrating agreement to better than 20%. The case of principal interest is shown in the lower graph, behind the first reflected shock where most of the present spectroscopic work is done. Refined calculations and measurements will enable much more precise comparisons, both here and in upper graph where predicted temperature is rough approximation.

Figure 8 Sequential image dissector (squid) for precise partition of spectral line profiles into narrow wavelength bands. Particular use for H_β profiles is indicated schematically. This method of joining glasses to light-pipes used in second model of squid.

Figure 9 Wavelength scan over H_β-profile in a set of similar experiments, using only one squid channel for preliminary tests. Theoretical profile shows expected nature of result.

Figure 10 Typical H_β-profiles from two shock tube experiments, using first model of multi-channel squid. Scaling the observations to the theoretical shapes as indicated gives agreement in electron densities to 20% or better. The error bars shown here arise from calibration difficulties, due in turn to details of light-pipe termination and consequent sensitivity to angular properties of illumination. Second model of squid (Figure8) superior in many respects.

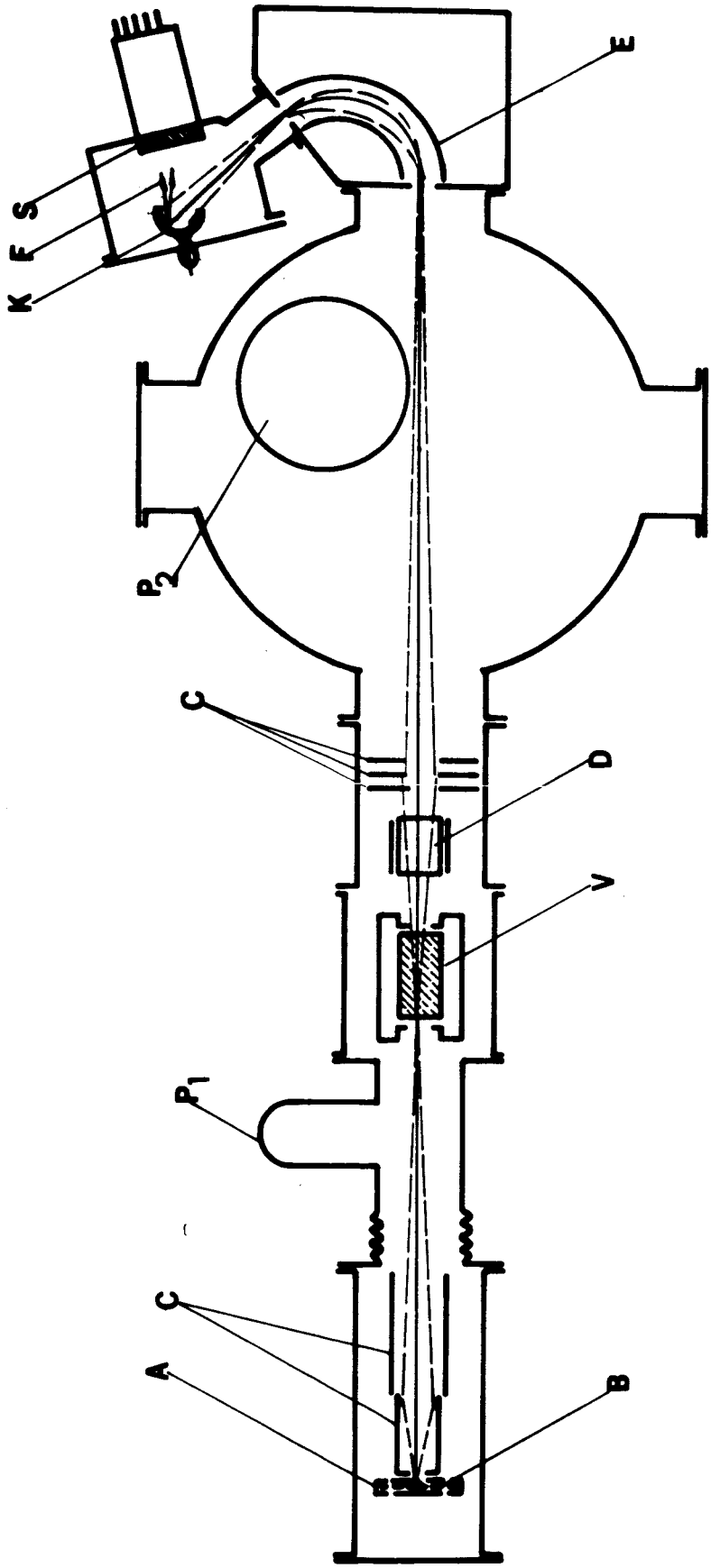
E
K
F
S
P2
C
D
V
P1
C
A
B

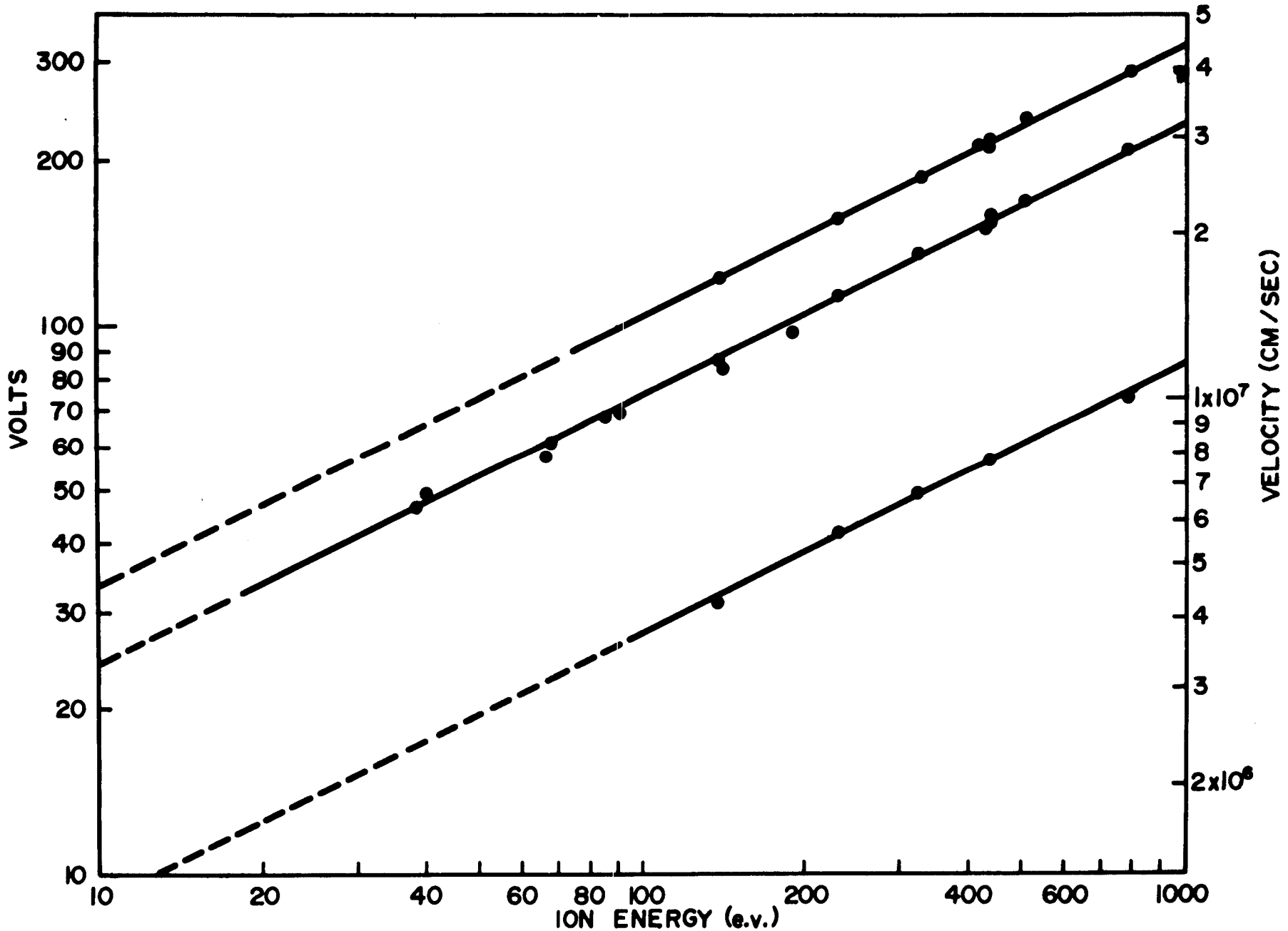
VOLTS
300
200
100
90
80
70
60
50
40
30
20
10
10
20
40
60
80
100
200
400
600
1000
ION ENERGY (e.v.)
5
4
3
2
1x10⁷
9
8
7
6
5
4
3
2x10⁶
VELOCITY (CM/SEC)

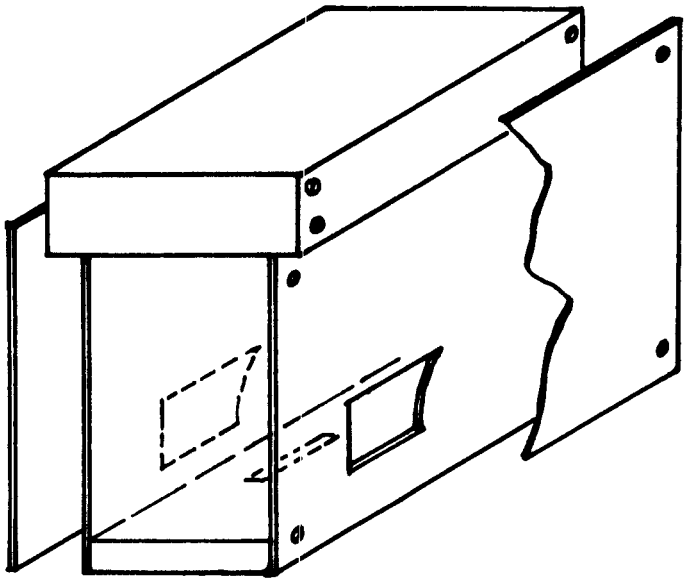

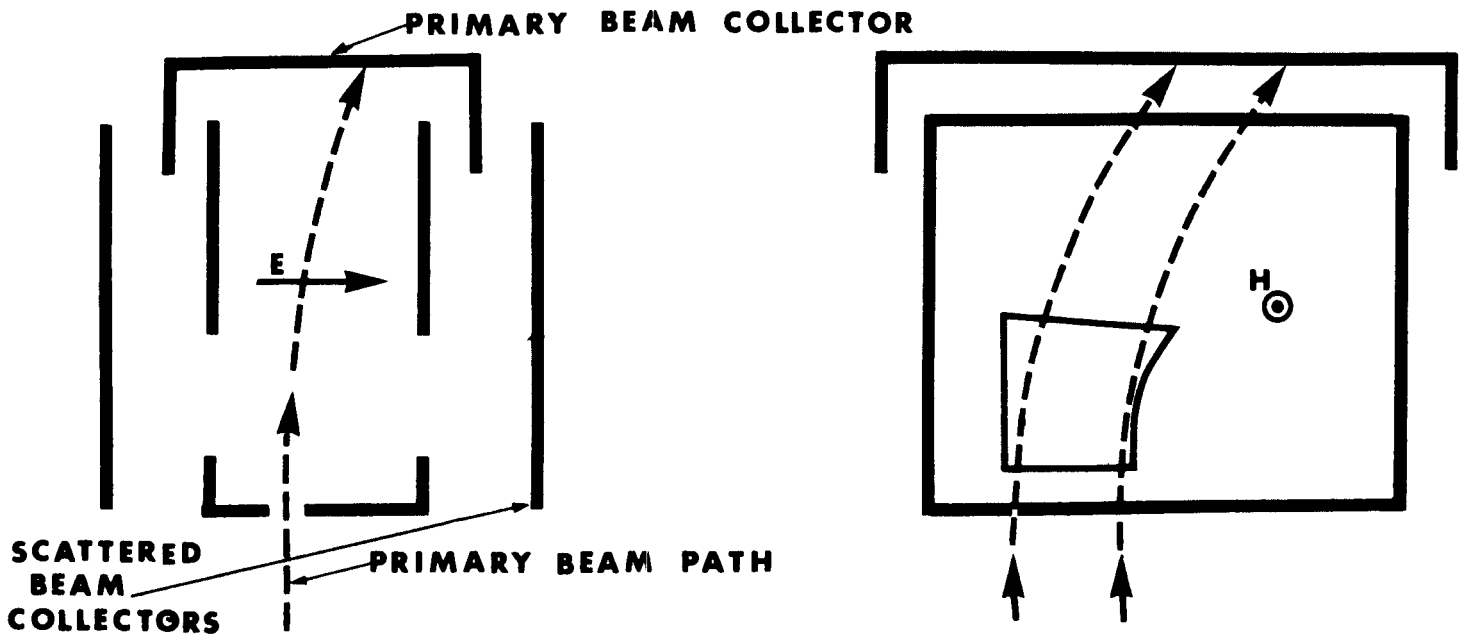
PRIMARY BEAM COLLECTOR
E
H
SCATTERED BEAM COLLECTORS
PRIMARY BEAM PATH

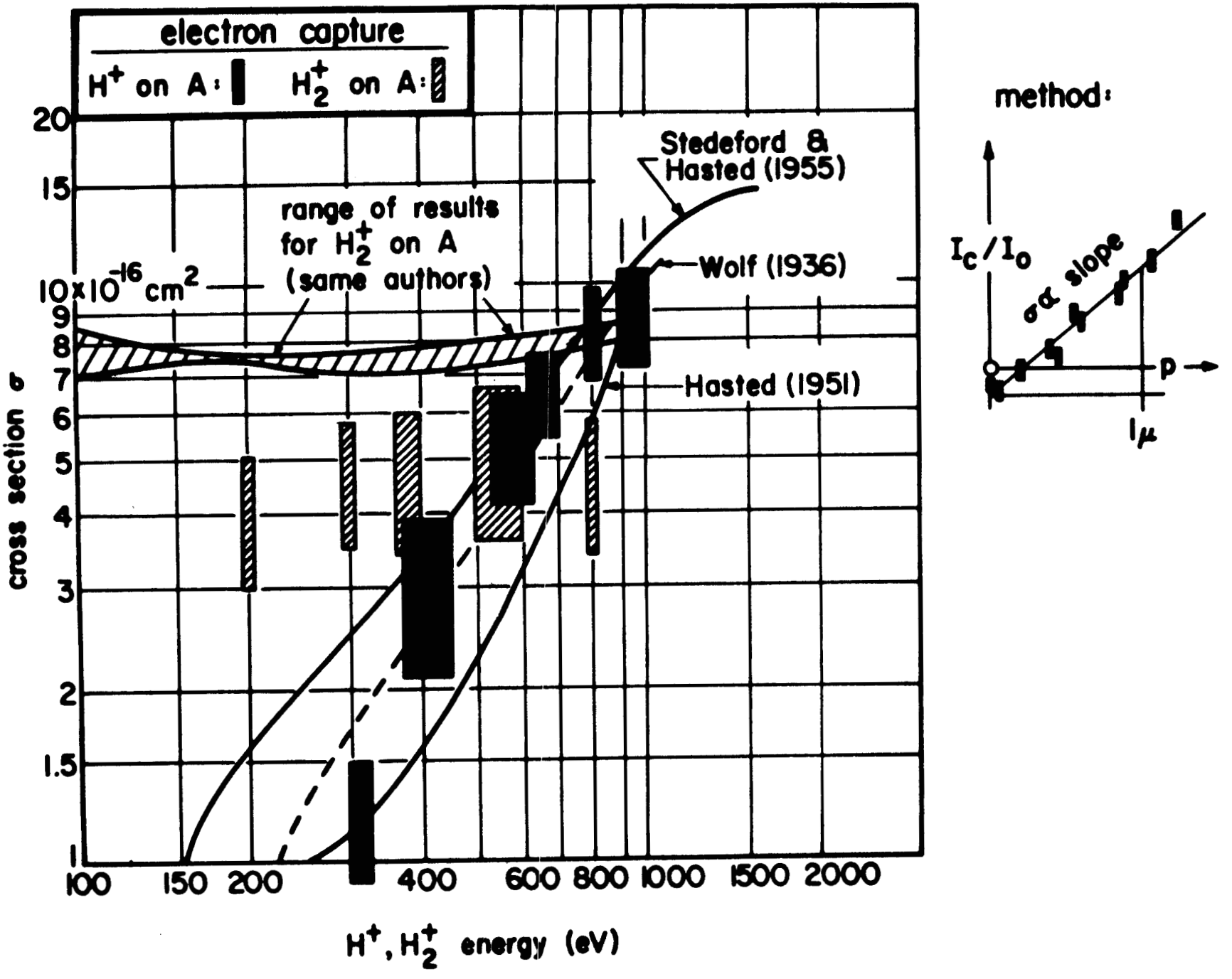
electron capture
H+ on A:
H2+ on A:
Stedeford & Hasted (1955)
range of results for H2+ on A (same authors)
Wolf (1936)
Hasted (1951)
10x10-16 cm2
cross section σ
20
15
10
9
8
7
6
5
4
3
2
1.5
1
100
150
200
400
600
800
1000
1500
2000
H+, H2+ energy (eV)
method:
Ic / Io
σ∝ slope
p
Iμ

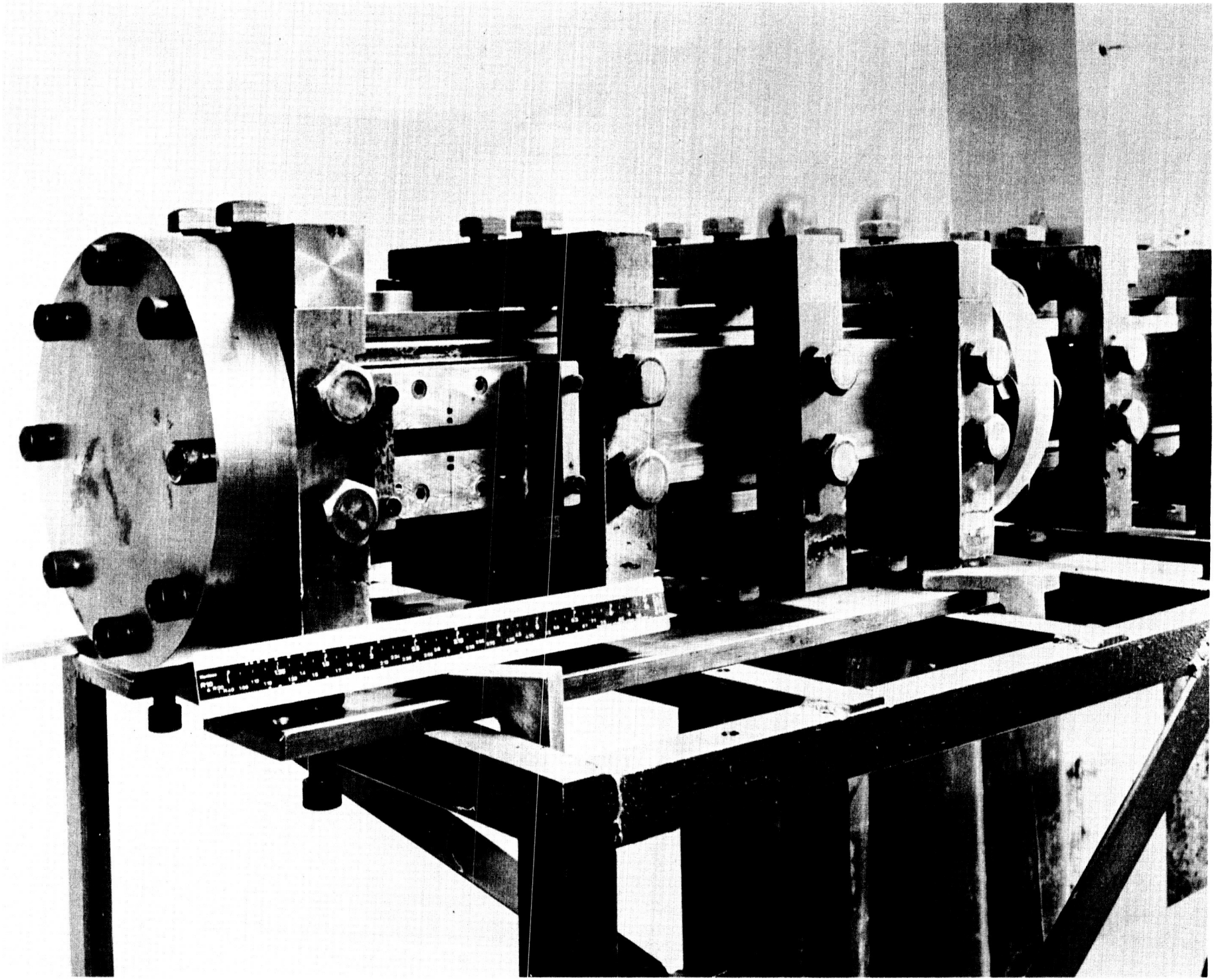

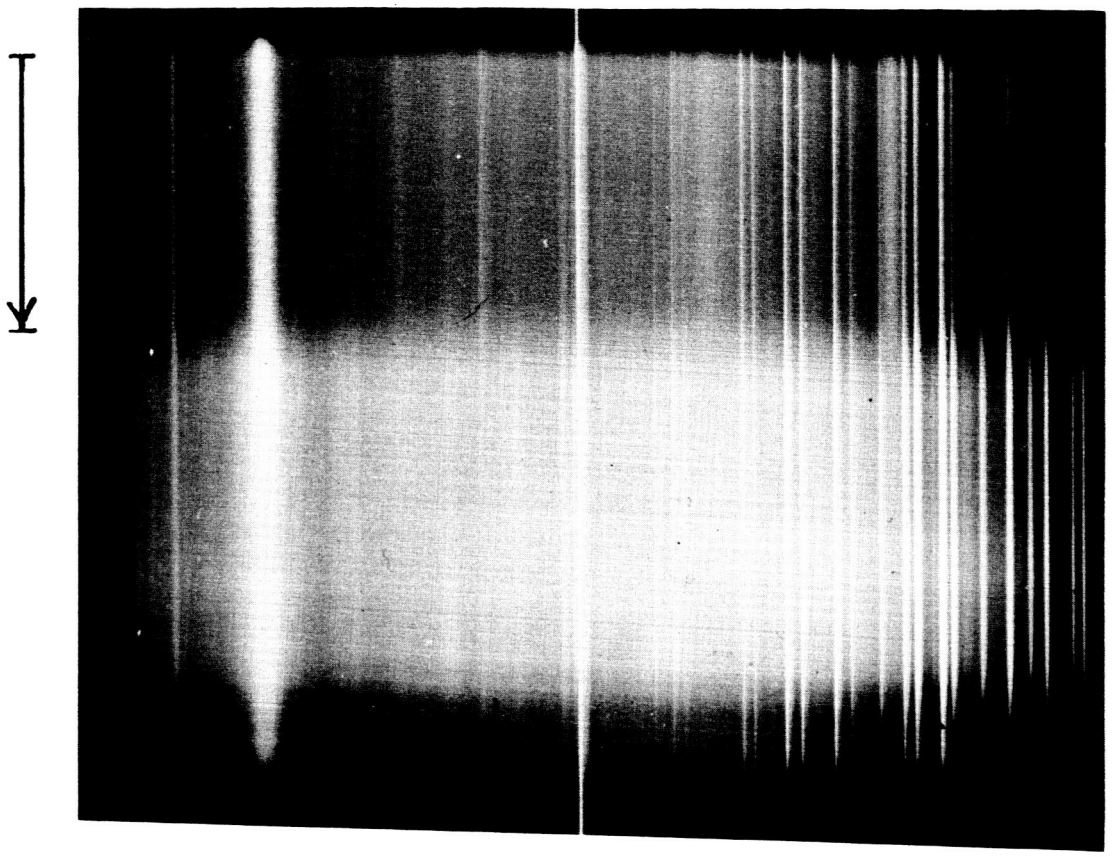

H_β • 4861

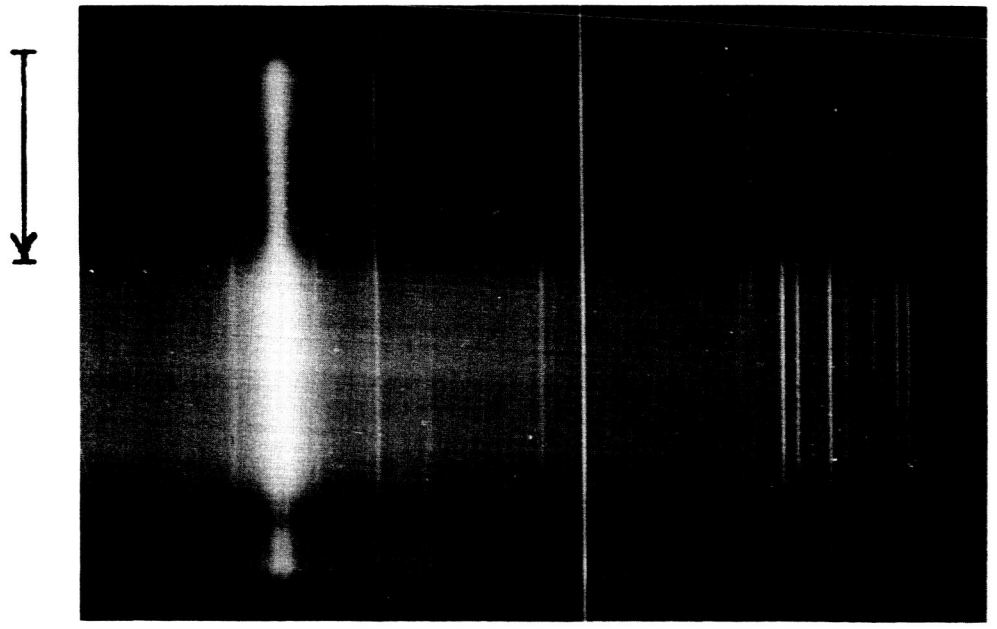

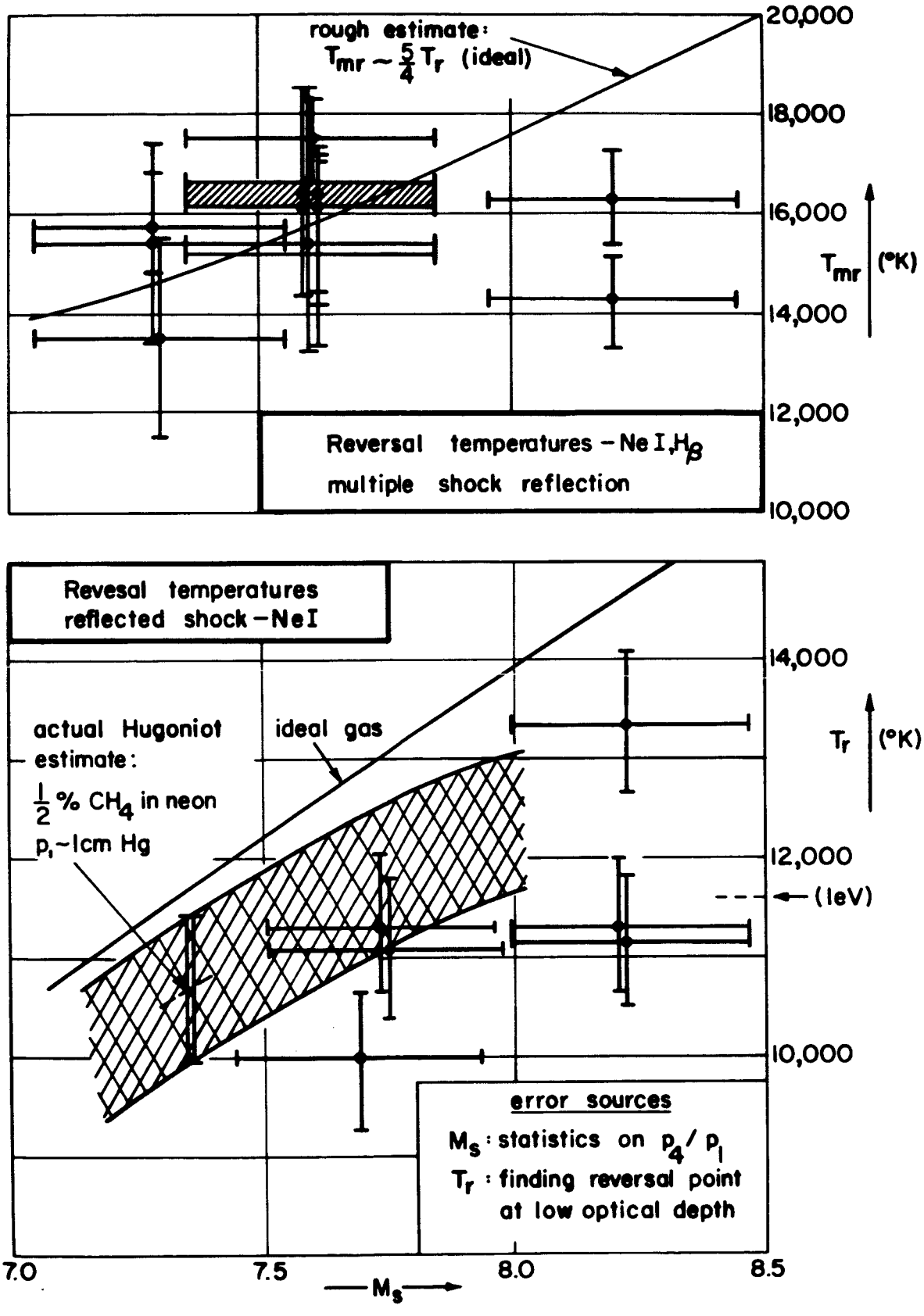
rough estimate:
$T_{mr} \sim \frac{5}{4} T_r$ (ideal)
20,000
18,000
16,000
14,000
12,000
10,000
T_{mr} (°K)
Reversal temperatures – Ne I, H_β
multiple shock reflection
Revesal temperatures
reflected shock – NeI
actual Hugoniot
estimate:
$\frac{1}{2}$ % CH_4 in neon
p_1 ~ 1cm Hg
ideal gas
14,000
12,000
10,000
T_r (°K)
(1eV)
error sources
M_s : statistics on p_4 / p_1
T_r : finding reversal point
at low optical depth
7.0
7.5
8.0
8.5
M_s

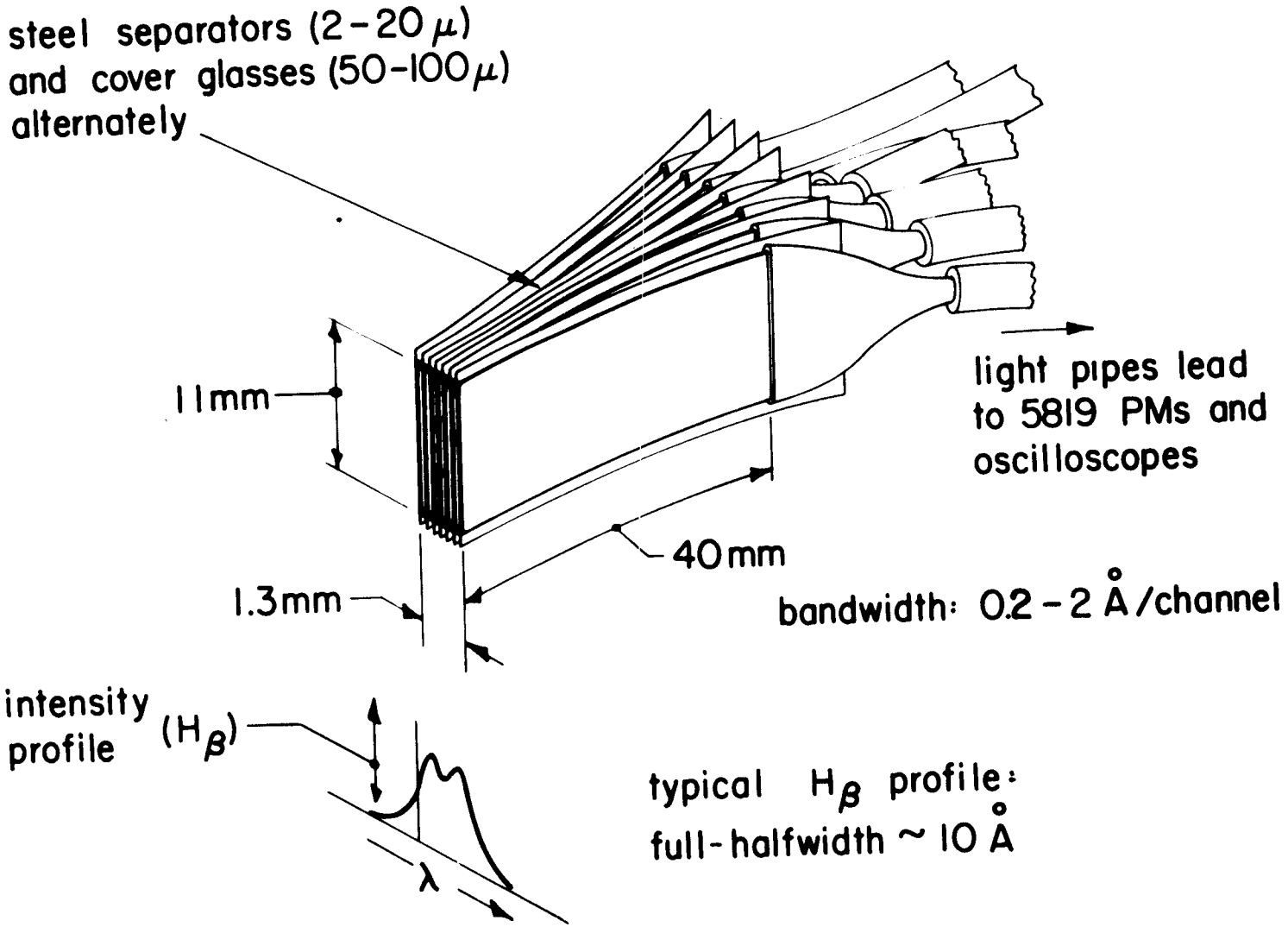
steel separators (2-20 μ)
and cover glasses (50-100 μ)
alternately
11mm
1.3mm
40mm
light pipes lead
to 5819 PMs and
oscilloscopes
bandwidth: 0.2 - 2 Å/channel
intensity
profile
(Hβ)
λ
typical Hβ profile:
full-halfwidth ~ 10 Å

SINGLE-CHANNEL SCAN OF H_β, EIGHT EXPERIMENTS

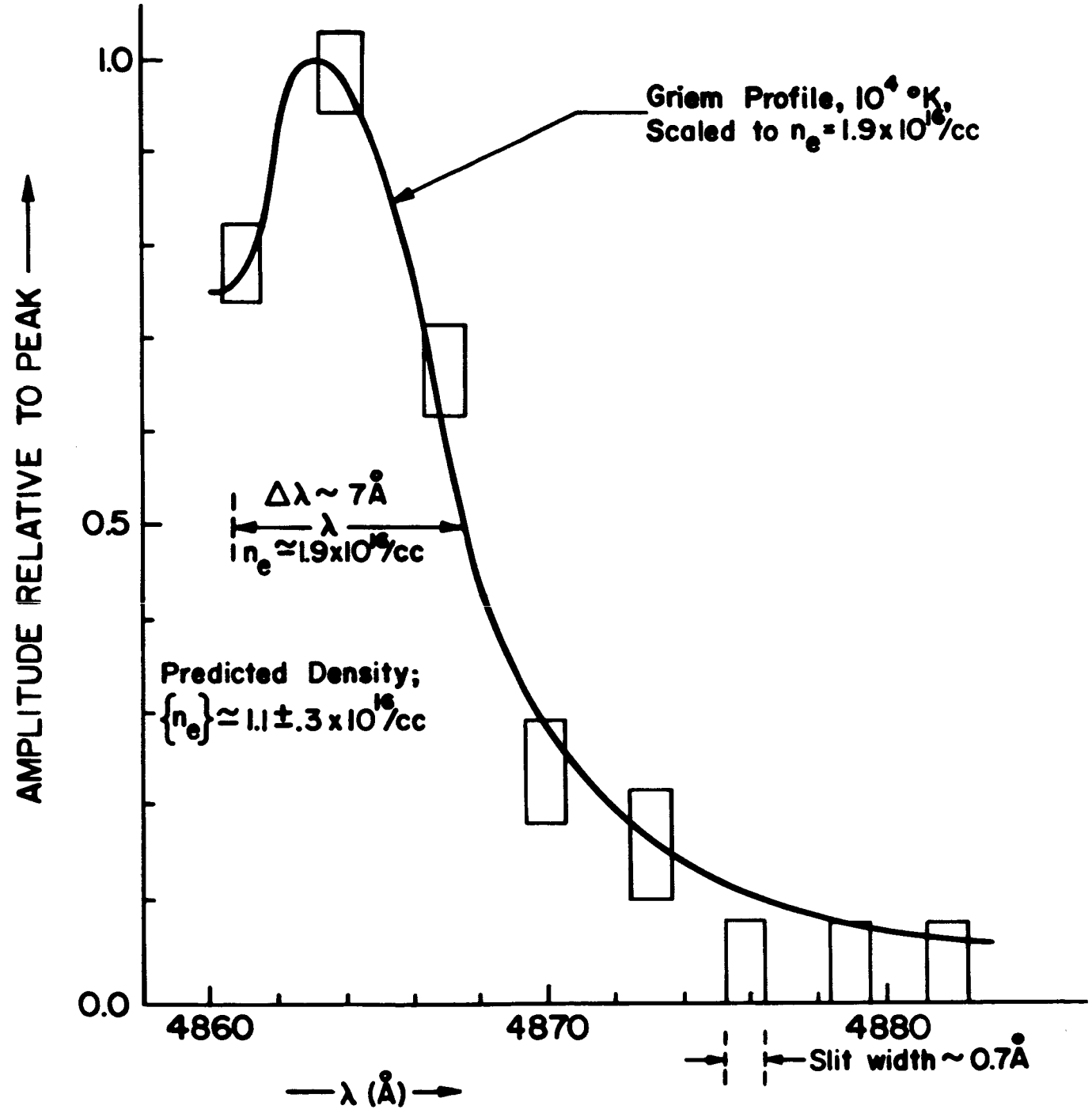

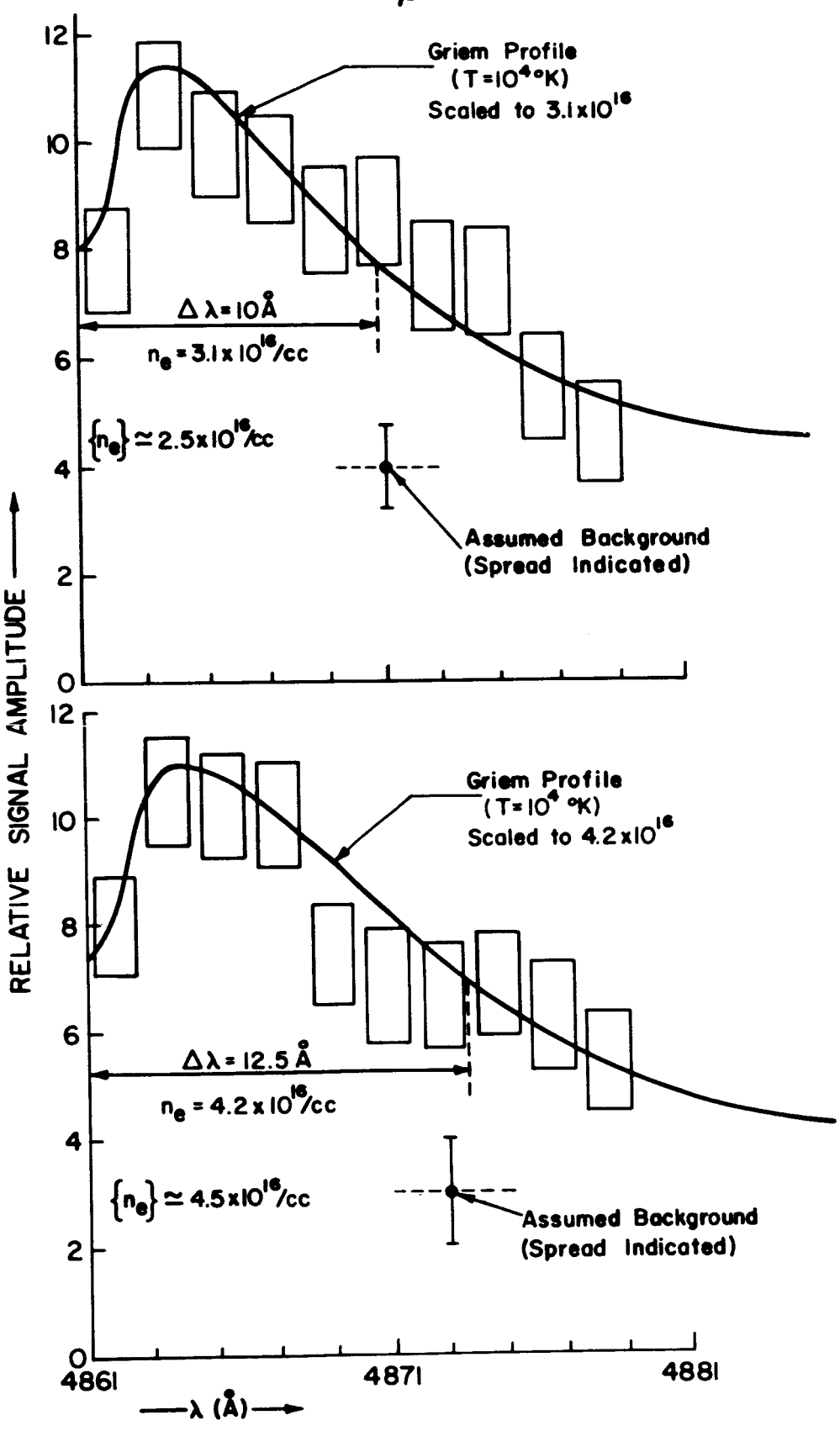
MULTICHANNEL SQUID, H_β, TWO EXPERIMENTS
Griem Profile
(T=10⁴°K)
Scaled to 3.1x10¹⁶
Δλ=10Å
n_e=3.1x10¹⁶/cc
{n_e} ≃ 2.5x10¹⁶/cc
Assumed Background
(Spread Indicated)
Griem Profile
(T=10⁴ °K)
Scaled to 4.2x10¹⁶
Δλ=12.5 Å
n_e = 4.2x10¹⁶/cc
{n_e} ≃ 4.5x10¹⁶/cc
Assumed Background
(Spread Indicated)
RELATIVE SIGNAL AMPLITUDE
0
2
4
6
8
10
12
4861
4871
4881
λ (Å)